

# Parallelization of continuous and discontinuous Galerkin dual-primal Isogeometric tearing and interconnecting methods

Christoph Hofer

*Johannes Kepler University (JKU), Altenbergerstr. 69, A-4040 Linz, Austria*

---

## Abstract

In this paper we investigate the parallelization of dual-primal isogeometric tearing and interconnecting (IETI-DP) type methods for solving large-scale continuous and discontinuous Galerkin systems of equations arising from Isogeometric analysis of elliptic boundary value problems. These methods are extensions of the finite element tearing and interconnecting methods to isogeometric analysis. The algorithms are implemented by means of energy minimizing primal subspaces. We discuss how these methods can efficiently be parallelized in a distributed memory setting. Weak and strong scaling studies presented for two and three dimensional problems show an excellent parallel efficiency.

*Keywords:* Diffusion problems, Isogeometric analysis, discontinuous Galerkin, IETI-DP, parallelization, MPI

---

## 1. Introduction

Isogeometric Analysis (IgA) is a novel methodology for the numerical solution of partial differential equations (PDE). IgA was first introduced by Hughes, Cottrell and Bazilevs in [24], see also the monograph [7] for a comprehensive presentation of the IgA framework and the recent survey article [3]. The main principle is to use the same basis functions for describing the geometry and to represent the discrete solution of the PDE problem under consideration. The most common choices are B-Splines, Non Uniform Rational B-Splines (NURBS), T-Splines, Truncated Hierarchical B-Splines (THB-Splines), etc., see, e.g., [15], [16] and [2]. One of the strengths of IgA is the capability of creating high-order splines spaces, while keeping the number of degrees of freedom quite small. Moreover, having basis functions with high smoothness is useful when considering higher-order PDEs, e.g., the biharmonic equation.

In many cases the domain can not be represented with a single mapping, referred to as *geometrical mapping*. Complicated geometries are decomposed into simple domains, called *patches*, which are topologically equivalent to a cube. The set of patches forming the computational domain is called multipatch domain. The obtained patch parametrizations and the original geometry may not be identical. The result are small gaps and overlaps occurring at the interfaces of the patches, called *segmentation crimes*, see [25], [41] and [23] for a comprehensive analysis. Nevertheless, one still wants to solve PDEs on such domains. To do so, numerical schemes based on the discontinuous Galerkin (dG) method for elliptic PDEs were developed in [20], [22] and [21]. There, the corresponding error analysis is also

provided. In addition to domains with segmentation crimes, the dG formulation is very useful when considering different B-Splines spaces on each patch, e.g., non-matching grids at the interface and different spline degrees. An analysis for the dG-IgA formulation with extensions to low regularity solutions can be found in [37]. For a detailed discussion of dG for finite element methods, we refer, e.g., to [44] and [8].

In the present paper, we are considering fast solution methods for linear systems arising from the discretization of elliptic PDEs by means of IgA. We investigate non-overlapping domain decomposition (DD) methods of the dual-primal tearing and interconnecting type. This type of methods are equivalent to the so called Balancing Domain Decomposition by Constraints (BDDC) methods, see [39], [45], [42] and references therein. The version based on a conforming Galerkin (cG) discretization, called dual-primal isogeometric tearing and interconnecting (IETI-DP) method was first introduced in [34] and the equivalent IgA BDDC method was analysed in [5]. Further extensions to the analysis are presented in [18]. The version based on the dG formulation, abbreviated by dG-IETI-DP, was introduced in [19], see [12], [13] and [14] for the corresponding finite element counterparts. We also want to mention development in overlapping Schwarz methods, see, e.g., [4] and [6]. The aim of this paper is to present the parallel scalability of the cG and dG IETI-DP methods. We investigate weak and strong scaling in two and three dimensional domains for different B-Spline degrees. The implemented algorithms are based on energy minimizing primal subspaces, which simplifies the parallelization of the solver part, but having more effort in the setup phase (assembling phase). We rephrase key parts of this algorithm and discuss how to realize the communication by means of Message Passing Interface (MPI). In general, FETI-DP and equivalent BDDC methods are by nature well suited for large-scale parallelization and has been widely studied for solving large-scale finite element equations, e.g., in [32], [43], [30] and [27], see also [29] for a hybrid OpenMP/MPI version. Considering a domain decomposition with several ten thousands of subdomains, the influence of the coarse grid problem becomes more and more significant. Especially, its LU-factorization is the bottleneck of the algorithm. The remedy is to reformulate the FETI-DP system in such a way that the solution of the coarse grid problem is not required in the application of the system matrix, but in the preconditioner. This enables the use of inexact methods like geometric or algebraic multigrid, see, e.g., [28], [27], [31], [32] and [33]. Moreover, inexact solvers can also be used in the scaled Dirichlet preconditioner and, if using the saddle point formulation, also for the local solvers, cf., [31], see also [32], [43] and references therein for alternative approaches by means of hybrid FETI. We also want to mention inexact version for the BDDC method, see, e.g., [46], [47], [10], [38] and [48]. FETI-DP methods has also been successfully applied to non-linear problems my means of a non-linear version of FETI-DP. We want to highlight recent advances presented, e.g., in [26], [28] and [27], showing excellent scalability on large-scale supercomputers.

In the present paper, we consider the following second-order elliptic boundary value problem in a bounded Lipschitz domain  $\Omega \subset \mathbb{R}^d$ , with  $d \in \{2, 3\}$ : Find  $u : \bar{\Omega} \rightarrow \mathbb{R}$  such that

$$-\operatorname{div}(\alpha \nabla u) = f \text{ in } \Omega, \quad u = 0 \text{ on } \Gamma_D, \quad \text{and } \alpha \frac{\partial u}{\partial n} = g_N \text{ on } \Gamma_N, \quad (1)$$

with given, sufficient smooth data  $f, g_N$  and  $\alpha$ , where the coefficient  $\alpha$  is uniformly bounded from below and above by some positive constants  $\alpha_{min}$  and  $\alpha_{max}$ , respectively. The boundary  $\partial\Omega$  of the computational domain  $\Omega$  consists of a Dirichlet part  $\Gamma_D$  of positive boundary measure and a Neumann part  $\Gamma_N$ . Furthermore, we assume that the Dirichlet boundary  $\Gamma_D$  is always a union of complete patch sides (edges / face in 2D /

3D) which are uniquely defined in IgA. Without loss of generality, we assume homogeneous Dirichlet conditions. This can always be obtained by homogenization. By means of integration by parts, we arrive at the weak formulation of (1) which reads as follows: Find  $u \in V_D = \{u \in H^1 : \gamma_0 u = 0 \text{ on } \Gamma_D\}$  such that

$$a(u, v) = \langle F, v \rangle \quad \forall v \in V_D, \quad (2)$$

where  $\gamma_0$  denotes the trace operator. The bilinear form  $a(\cdot, \cdot) : V_D \times V_D \rightarrow \mathbb{R}$  and the linear form  $\langle F, \cdot \rangle : V_D \rightarrow \mathbb{R}$  are given by the expressions

$$a(u, v) := \int_{\Omega} \alpha \nabla u \cdot \nabla v \, dx \quad \text{and} \quad \langle F, v \rangle := \int_{\Omega} f v \, dx + \int_{\Gamma_N} g_N v \, ds.$$

70 The remainder of the paper is organized as follows: In Section 2, we give a short intro-  
 71 duction to isogeometric analysis, providing the basic definitions and notations. Section 3  
 72 describes the different discretizations of the model problem obtained the continuous and  
 73 discontinuous Galerkin methods. In Section 4, we formulate the IETI-DP method for  
 74 both discretizations and provide implementation details. The way how the algorithm is  
 75 parallelized is explained in Section 5. Numerical examples are presented in Section 6.  
 76 Finally we draw some conclusions in Section 7.

## 77 2. Isogeometric Analysis

78 In this section, we give a very short overview about IgA. For a more comprehensive study,  
 79 we refer to, e.g., [7] and [37].

80 Let  $\hat{\Omega} := (0, 1)^d, d \in \{2, 3\}$ , be the d-dimensional unit cube, which we refer to as the  
 81 *parameter domain*. Let  $p_\iota$  and  $M_\iota, \iota \in \{1, \dots, d\}$ , be the B-Spline degree and the number  
 82 of basis functions in  $x_\iota$ -direction. Moreover, let  $\Xi_\iota = \{\xi_1 = 0, \xi_2, \dots, \xi_{n_\iota} = 1\}, n_\iota =$   
 83  $M_\iota - p_\iota - 1$ , be a partition of  $[0, 1]$ , called *knot vector*. With this ingredients we are able  
 84 to define the B-Spline basis  $\hat{N}_{i,p}, i \in \{1, \dots, M_\iota\}$  on  $[0, 1]$  via Cox-De Boor's algorithm,  
 85 cf. [7]. The generalization to  $\hat{\Omega}$  is realized by considering a tensor product, again denoted  
 86 by  $\hat{N}_{i,p}$ , where  $i = (i_1, \dots, i_d)$  and  $p = (p_1, \dots, p_d)$  are a multi-indices. For notational  
 87 simplicity, we define  $\mathcal{I} := \{(i_1, \dots, i_d) \mid i_\iota \in \{1, \dots, M_\iota\}\}$  as the set of multi-indices. Since  
 88 the tensor product knot vector  $\Xi$  provides a partition of  $\hat{\Omega}$ , it introduces a mesh  $\hat{\mathcal{Q}}$ , and  
 89 we denote a mesh element by  $\hat{Q}$ , called *cell*.

The B-Spline basis functions parametrize the computational domain  $\Omega$ , also called *physical domain*. It is given as image of parameter domain under the *geometrical mapping*  $G : \hat{\Omega} \rightarrow \mathbb{R}^d$ , defined as

$$G(\xi) := \sum_{i \in \mathcal{I}} P_i \hat{N}_{i,p}(\xi),$$

90 with the control points  $P_i \in \mathbb{R}^d, i \in \mathcal{I}$ . The image of the mesh  $\hat{\mathcal{Q}}_h$  under  $G$  defines  
 91 the mesh on  $\Omega$ , denoted by  $\mathcal{Q}_h$  with cells  $Q$ . Both meshes possess a characteristic mesh  
 92 size  $\hat{h}$  and  $h$ , respectively. More complicated geometries  $\Omega$  have to be represented with  
 93 multiple non-overlapping domains  $\Omega^{(k)} := G^{(k)}(\hat{\Omega}), k = 1, \dots, N$ , called *patches*, where  
 94 each patch is associated with a different geometrical mapping  $G^{(k)}$ . We sometimes call  
 95  $\bar{\Omega} := \bigcup_{k=1}^N \bar{\Omega}^{(k)}$  a *multipatch domain*. Furthermore, we denote the set of all indices  $l$  such

96 that  $\Omega^{(k)}$  and  $\Omega^{(l)}$  have a common interface  $F^{(kl)}$  by  $\mathcal{I}_{\mathcal{F}}^{(k)}$ . We define the interface  $\Gamma^{(k)}$  of  
 97  $\Omega^{(k)}$  as  $\Gamma^{(k)} := \bigcup_{l \in \mathcal{I}_{\mathcal{F}}^{(k)}} F^{(kl)}$ .

We use B-Splines not only for defining the geometry, but also for representing the approximate solution of our PDE. This motivates to define the basis functions in the physical space  $N_{i,p} := \hat{N}_{i,p} \circ G^{-1}$  and the corresponding discrete space as

$$V_h := \text{span}\{N_{i,p}\}_{i \in \mathcal{I}}. \quad (3)$$

98 Moreover, each function  $u_h(x) = \sum_{i \in \mathcal{I}} u_i N_{i,p}(x)$  is associated with the coefficient vector  
 99  $\mathbf{u} = (u_i)_{i \in \mathcal{I}}$ . This map is known as *Ritz isomorphism* or *IgA isomorphism* in connection  
 100 with IgA. One usually writes this relation as  $u_h \leftrightarrow \mathbf{u}$ . In the following, we will use the  
 101 notation  $u_h$  for the function and its vector representations. If we consider a single patch  
 102  $\Omega^{(k)}$  of a multipatch domain  $\Omega$ , we will use the notation  $V_h^{(k)}$ ,  $N_{i,p}^{(k)}$ ,  $\hat{N}_{i,p}^{(k)}$ ,  $G^{(k)}$ ,  $\dots$  with the  
 103 analogous definitions. To keep notation simple, we will use  $h_k$  and  $\hat{h}_k$  instead of  $h^{(k)}$  and  
 104  $\hat{h}^{(k)}$ , respectively.

### 105 3. Galerkin Methods for Isogeometric Analysis

106 In this section we rephrase the variational formulation for the continuous and discontinuous  
 107 Galerkin method for multipatch IgA systems.

#### 108 3.1. Continuous Galerkin method

We are considering the finite dimensional subspace  $V_h^{cG}$  of  $V_D$ , where  $V_h^{cG}$  is given by

$$V_h^{cG} := \{v \mid v|_{\Omega^{(k)}} \in V_h^{(k)}\} \cap H^1(\Omega).$$

Since, we restrict ourselves to homogeneous Dirichlet conditions, we look for the Galerkin approximate  $u_h$  from  $V_{D,h}^{cG} \subset V_h^{cG}$ , where  $V_{D,h}^{cG}$  contains all functions, which vanish on the Dirichlet boundary. The Galerkin IgA scheme reads as follows: Find  $u_h \in V_{D,h}^{cG}$  such that

$$a(u_h, v_h) = \langle F, v_h \rangle \quad \forall v_h \in V_{D,h}. \quad (4)$$

109 There exists a unique IgA solution  $u_h \in V_{D,h}^{cG}$  of (4) that converges to the solution  $u \in V_D$   
 110 of (2) if  $h$  tends to 0. Due to Cea's lemma, the usual discretization error estimates in the  
 111  $H^1$  - norm follow from the corresponding approximation error estimates, see [1] or [3].

#### 112 3.2. Discontinuous Galerkin method

In the dG-IgA scheme, we again use the spaces  $V_h^{(k)}$  of B-Splines defined in (3), whereas now discontinuities are allowed across the patch interfaces  $F^{(kl)}$ . The continuity of the function value and its normal fluxes are then enforced in a weak sense by adding additional terms to the bilinear form. We define the dG-IgA space

$$V_h^{dG} := \{v \mid v|_{\Omega^{(k)}} \in V_h^{(k)}\}, \quad (5)$$

where  $V_h^{(k)}$  is defined as in (3). A comprehensive study of dG schemes for FE can be found in [44] and [8]. For an analysis of the dG-IgA scheme, we refer to [37]. We define  $V_{D,h}^{dG}$  as the space of all functions from  $V_h$  that vanish on the Dirichlet boundary  $\Gamma_D$ . Having these

definitions at hand, we can define the discrete problem based on the Symmetric Interior Penalty (SIP) dG formulation as follows: Find  $u_h \in V_{D,h}^{dG}$  such that

$$a_h(u_h, v_h) = \langle F, v_h \rangle \quad \forall v_h \in V_{D,h}^{dG}, \quad (6)$$

where

$$a_h(u, v) := \sum_{k=1}^N a_e^{(k)}(u, v) \quad \text{and} \quad \langle F, v \rangle := \sum_{k=1}^N \left( \int_{\Omega^{(k)}} f v^{(k)} dx + \int_{\Gamma_N^{(k)}} g_N v^{(k)} ds \right),$$

$$a_e^{(k)}(u, v) := a^{(k)}(u, v) + s^{(k)}(u, v) + p^{(k)}(u, v),$$

and

$$a^{(k)}(u, v) := \int_{\Omega^{(k)}} \alpha^{(k)} \nabla u^{(k)} \nabla v^{(k)} dx,$$

$$s^{(k)}(u, v) := \sum_{l \in \mathcal{I}_{\mathcal{F}}^{(k)}} \int_{F^{(kl)}} \frac{\alpha^{(k)}}{2} \left( \frac{\partial u^{(k)}}{\partial n} (v^{(l)} - v^{(k)}) + \frac{\partial v^{(k)}}{\partial n} (u^{(l)} - u^{(k)}) \right) ds,$$

$$p^{(k)}(u, v) := \sum_{l \in \mathcal{I}_{\mathcal{F}}^{(k)}} \int_{F^{(kl)}} \frac{\delta \alpha^{(k)}}{h_{kl}} (u^{(l)} - u^{(k)}) (v^{(l)} - v^{(k)}) ds.$$

- 113 Here the notation  $\frac{\partial}{\partial n}$  denotes the derivative in the direction of the outer normal vector,  
 114  $\delta$  a positive sufficiently large penalty parameter, and  $h_{kl}$  the harmonic average of the  
 115 adjacent mesh sizes, i.e.,  $h_{kl} = 2h_k h_l / (h_k + h_l)$ .

We equip  $V_{D,h}^{dG}$  with the dG-norm

$$\|u\|_{dG}^2 = \sum_{k=1}^N \left[ \alpha^{(k)} \|\nabla u^{(k)}\|_{L^2(\Omega^{(k)})}^2 + \sum_{l \in \mathcal{I}_{\mathcal{F}}^{(k)}} \frac{\delta \alpha^{(k)}}{h_{kl}} \int_{F^{(kl)}} (u^{(k)} - u^{(l)})^2 ds \right]. \quad (7)$$

Furthermore, we define the bilinear forms

$$d_h(u, v) = \sum_{k=1}^N d^{(k)}(u, v) \quad \text{where} \quad d^{(k)}(u, v) = a^{(k)}(u, v) + p^{(k)}(u, v),$$

- 116 for later use. We note that  $\|u_h\|_{dG}^2 = d_h(u_h, u_h)$ .

**Lemma 3.1.** *Let  $\delta$  be sufficiently large. Then there exist two positive constants  $\gamma_0$  and  $\gamma_1$ , which are independent of  $h_k, H_k, \delta, \alpha^{(k)}$  and  $u_h$  such that the inequalities*

$$\gamma_0 d^{(k)}(u_h, u_h) \leq a_e^{(k)}(u_h, u_h) \leq \gamma_1 d^{(k)}(u_h, u_h), \quad \forall u_h \in V_{D,h}^{dG} \quad (8)$$

are valid for all  $k = 1, 2, \dots, N$ . Furthermore, we have the inequalities

$$\gamma_0 \|u_h\|_{dG}^2 \leq a_h(u_h, u_h) \leq \gamma_1 \|u_h\|_{dG}^2, \quad \forall u_h \in V_{D,h}^{dG}. \quad (9)$$

- 117 This Lemma is an equivalent statement of Lemma 2.1 in [13] for IgA, and the proof can  
 118 be found in [19]. A direct implication of (9) is the well posedness of the discrete problem

119 (6) by the Theorem of Lax-Milgram. The consistency of the method together with the  
 120 interpolation estimates of B-Splines lead to the a-priori error estimate, established in [37].  
 121 We note that, in [37], the results were obtained for the Incomplete Interior Penalty (IIP)  
 122 scheme. An extension to SIP-dG and the use of harmonic averages for  $h$  and/or  $\alpha$  are  
 123 discussed in Remark 3.1 in [37], see also [36].

For both the cG and dG formulation, we choose the B-Spline function  $\{N_{i,p}\}_{i \in \mathcal{I}_0}$  as basis for the space  $V_h^X$ ,  $X \in \{cG, dG\}$ , where  $\mathcal{I}_0$  contains all indices of  $\mathcal{I}$ , where the corresponding basis functions do not have a support on the Dirichlet boundary. In the cG case, the basis functions on the interface are identified accordingly to obtain a conforming subspace of  $V_D$ . For the remainder of this paper, we drop the superscript  $X \in \{cG, dG\}$  and use the symbol  $V_h$  for both formulations. Depending on the considered formulation, one needs to use the right space  $V_h^X$ ,  $X \in \{cG, dG\}$ . The IgA schemes (4) and (6) are equivalent to the system of linear IgA equations

$$\mathbf{K}\mathbf{u} = \mathbf{f}, \quad (10)$$

124 where  $\mathbf{K} = (\mathbf{K}_{i,j})_{i,j \in \mathcal{I}_0}$ ,  $\mathbf{f} = (\mathbf{f}_i)_{i \in \mathcal{I}_0}$  denote the stiffness matrix and the load vector,  
 125 respectively, with  $\mathbf{K}_{i,j} = a(N_{j,p}, N_{i,p})$  or  $\mathbf{K}_{i,j} = a_h(N_{j,p}, N_{i,p})$  and  $\mathbf{f}_i = \langle F, N_{i,p} \rangle$ , and  $\mathbf{u}$   
 126 is the vector representation of  $u_h$ .

## 127 4. IETI-DP methods and their implementation

128 In this section, we recall the main ingredients for the cG-IETI-DP and dG-IETI-DP  
 129 method. We focus mainly on the implementation, since this is the relevant part for  
 130 parallelization.

### 131 4.1. Derivation of the method

132 A rigorous and formal definition of the cG-IETI-DP and dG-IETI-DP method is quite  
 133 technical and not necessary for the parallelization, which is the purpose of this paper.  
 134 Therefore, we are not going to present the whole derivation of each method. We will give  
 135 a general description, which is valid for both methods. For a detailed derivation, we refer  
 136 to [18] and [19].

The first step is to introduce additional dofs on the interface to decouple the local problems and incorporate their connection via Lagrange multipliers  $\boldsymbol{\lambda}$ . This is quite straightforward in the case of the cG formulation, but more involved in the dG case. In any of the two cases, we can equivalently rewrite (10) as: Find  $(u, \boldsymbol{\lambda}) \in V_{h,e} \times U$  such that

$$\begin{bmatrix} K_e & B^T \\ B & 0 \end{bmatrix} \begin{bmatrix} u \\ \boldsymbol{\lambda} \end{bmatrix} = \begin{bmatrix} \mathbf{f} \\ 0 \end{bmatrix}, \quad (11)$$

where  $V_{h,e} \supset V_h$ , is the decoupled space with additional dofs and  $U$  is the set of Lagrange multipliers. The jump operator  $B$  enforces the ‘‘continuity’’ of the solution  $u$  in the sense that  $\ker(B) \equiv V_h$ . The matrix  $K_e$  is the block diagonal matrix of the patch local stiffness matrices  $K^{(k)}$ , i.e.,  $K_e = \text{diag}(K^{(k)})$ . Since  $B$  only acts on the patch interface dofs, we first can reorder the stiffness matrix in the following way

$$K^{(k)} = \begin{bmatrix} K_{BB}^{(k)} & K_{BI}^{(k)} \\ K_{IB}^{(k)} & K_{II}^{(k)} \end{bmatrix}, \quad \mathbf{f}^{(k)} = \begin{bmatrix} f_B^{(k)} \\ f_I^{(k)} \end{bmatrix}$$

and then consider only the Schur complement representation: Find  $(u_B, \boldsymbol{\lambda}) \in W \times U$  such that

$$\begin{bmatrix} S_e & B_B^T \\ B_B & 0 \end{bmatrix} \begin{bmatrix} u_B \\ \boldsymbol{\lambda} \end{bmatrix} = \begin{bmatrix} g \\ 0 \end{bmatrix}, \quad (12)$$

137 where  $S_e = \text{diag}(S_e^{(k)})$ ,  $S_e^{(k)} = K_{BB}^{(k)} - K_{BI}^{(k)}(K_{II}^{(k)})^{-1}K_{IB}^{(k)}$  and  $g^{(k)} = f_B - K_{BI}^{(k)}(K_{II}^{(k)})^{-1}f_I^{(k)}$ .  
 138 The space  $W$  is the restriction of  $V_{h,e}$  to the interface. For completeness, we denote its  
 139 “continuous” representation as  $\widehat{W}$ , i.e.,  $\ker(B_B) = \widehat{W}$ . Equation (12) is valid for the  
 140 cG-IETI-DP and dG-IETI-DP method, but the matrix  $K_e$  has difference entries and the  
 141 number of boundary dofs (subscript  $B$ ) is different. Fortunately, this does not change the  
 142 way how the algorithm is implemented and parallelized. In the following, we will drop  
 143 the subscript  $B$  in  $u_B$  and  $B_B$  for notational simplicity.

The matrix  $S_e$  is not invertible and, hence, we cannot build the Schur complement system of (12). To overcome this, we introduce an intermediate space  $\widetilde{W}$ , such that  $\widehat{W} \subset \widetilde{W} \subset W$ , and  $S_e$  restricted to  $\widetilde{W}$ , denoted by  $\widetilde{S}$ , is invertible. We introduce primal variables as a set  $\Psi \subset \widehat{W}^*$  and define the spaces

$$\widetilde{W} := \{w \in W : \psi(w^{(k)}) = \psi(w^{(l)}), \forall \psi \in \Psi, \forall k > l\}$$

and

$$W_\Delta := \prod_{k=1}^N W_\Delta^{(k)}, \quad \text{with} \quad W_\Delta^{(k)} := \{w^{(k)} \in W^{(k)} : \psi(w^{(k)}) = 0 \forall \psi \in \Psi\}.$$

144 Moreover, we introduce the space  $W_\Pi \subset \widehat{W}$  such that  $\widetilde{W} = W_\Pi \oplus W_\Delta$ . We call  $W_\Pi$  *primal*  
 145 *space* and  $W_\Delta$  *dual space*. Typically, the set  $\Psi$  corresponds to “continuous” vertex values,  
 146 edge averages and/or face averages.

Since  $\widetilde{W} \subset W$ , there is a natural embedding  $\widetilde{I} : \widetilde{W} \rightarrow W$ . Let the jump operator restricted to  $\widetilde{W}$  be  $\widetilde{B} := B\widetilde{I} : \widetilde{W} \rightarrow U^*$ . Now we are in the position to reformulate problem (12) in the space  $\widetilde{W}$  as follows: Find  $(u, \boldsymbol{\lambda}) \in \widetilde{W} \times U$ :

$$\begin{bmatrix} \widetilde{S} & \widetilde{B}^T \\ \widetilde{B} & 0 \end{bmatrix} \begin{bmatrix} u \\ \boldsymbol{\lambda} \end{bmatrix} = \begin{bmatrix} \widetilde{g} \\ 0 \end{bmatrix}, \quad (13)$$

147 where  $\widetilde{g} := \widetilde{I}^T g$ , and  $\widetilde{B}^T = \widetilde{I}^T B^T$ . Here,  $\widetilde{I}^T : W^* \rightarrow \widetilde{W}^*$  denotes the adjoint of  $\widetilde{I}$ .

By construction,  $\widetilde{S}$  is SPD on  $\widetilde{W}$ . Hence, we can define the Schur complement  $F$  and the corresponding right-hand side as follows:

$$F := \widetilde{B}\widetilde{S}^{-1}\widetilde{B}^T, \quad d := \widetilde{B}\widetilde{S}^{-1}\widetilde{g}.$$

Hence, the saddle point system (13) is equivalent to the Schur complement problem:

$$\text{Find } \boldsymbol{\lambda} \in U : \quad F\boldsymbol{\lambda} = d. \quad (14)$$

148 Equation (14) is solved by means of the PCG algorithm, but it requires an appropriate  
 149 preconditioner in order to obtain an efficient solver.

Recalling the definition of  $S_e = \text{diag}(S_e^{(k)})_{k=1}^N$ , we define the scaled Dirichlet preconditioner  $M_{sD}^{-1} := B_D S_e B_D^T$ , where  $B_D$  is a scaled version of the jump operator  $B$ . The scaled jump operator  $B_D$  is defined such that the operator enforces the constraints

$$\delta_j^{\dagger(l)}(\mathbf{u}^{(k)})_i^{(k)} - \delta_i^{\dagger(k)}(\mathbf{u}^{(l)})_j^{(k)} = 0 \quad \forall (i, j) \in B_e(k, l), \forall l \in \mathcal{I}_{\mathcal{F}}^{(k)},$$

and

$$\delta_j^{\dagger(l)}(\mathbf{u}^{(k)})_i^{(l)} - \delta_i^{\dagger(k)}(\mathbf{u}^{(l)})_j^{(l)} = 0 \quad \forall (i, j) \in B_e(l, k), \forall l \in \mathcal{I}_{\mathcal{F}}^{(k)},$$

where, for  $(i, j) \in B_e(k, l)$ ,  $\delta_i^{\dagger(k)} := \rho_i^{(k)} / \sum_{l \in \mathcal{I}_{\mathcal{F}}^{(k)}} \rho_j^{(l)}$  is an appropriate scaling. One can show, that the preconditioned system for the cG version has a quasi-optimal condition number bound with respect to  $H/h := \max_k(H_k/h_k)$ , i.e.,

$$\kappa(M_{sD}^{-1}F|_{\ker(\tilde{B}^T)}) \leq C(1 + \log(H/h))^2, \quad (15)$$

150 see [18] and [5]. Moreover, numerical examples show also robustness with respect to jumps  
151 in the diffusion coefficient and only a weak dependence on the B-Spline degree  $p$ , see, e.g.,  
152 [19], [18] and [5].

#### 153 4.2. Implementation of the algorithm

Since  $F$  is symmetric and positive definite on  $\tilde{U}$ , we can solve the linear system  $F\boldsymbol{\lambda} = d$  by means of the PCG algorithm, where we use  $M_{sD}^{-1}$  as preconditioner. The PCG does not require an explicit representation of the matrices  $F$  and  $M_{sD}^{-1}$ , since we just need their application to a vector. There are different ways to provide an efficient implementation. We will follow the concept of the energy minimizing primal subspaces. The idea is to split the space  $\tilde{W}$  into  $\tilde{W}_{\Pi} \oplus \prod \tilde{W}_{\Delta}^{(k)}$ , such that  $\tilde{W}_{\Delta}^{(k)} \perp_S \tilde{W}_{\Pi}$  for all  $k$ , i.e., we choose  $\tilde{W}_{\Pi} := \tilde{W}_{\Delta}^{\perp_S}$ , see, e.g., [42] and [9]. By means of this choice, the operators  $\tilde{S}$  and  $\tilde{S}^{-1}$  have the following forms

$$\tilde{S} = \begin{bmatrix} S_{\Pi\Pi} & 0 \\ 0 & S_{\Delta\Delta} \end{bmatrix} \quad \text{and} \quad \tilde{S}^{-1} = \begin{bmatrix} S_{\Pi\Pi}^{-1} & 0 \\ 0 & S_{\Delta\Delta}^{-1} \end{bmatrix},$$

154 where  $S_{\Pi\Pi}$  and  $S_{\Delta\Delta}$  are the restrictions of  $\tilde{S}$  to the corresponding subspaces. We note  
155 that  $S_{\Delta\Delta}$  can be seen as a block diagonal operator, i.e.,  $S_{\Delta\Delta} = \text{diag}(S_{\Delta\Delta}^{(k)})$ .

156 The application of  $F$  and  $M_{sD}^{-1}$  is summarized in Algorithm 1.

##### 157 4.2.1. Constructing a basis for the primal subspace

First we need to provide an appropriate local basis  $\{\tilde{\phi}_j\}_j^{n_{\Pi}}$  for  $\tilde{W}_{\Pi}$ , where  $n_{\Pi}$  is the number of primal variables. We request from the basis that it has to be nodal with respect to the primal variables, i.e.,  $\psi_i(\tilde{\phi}_j) = \delta_{i,j}$ , for  $i, j \in \{1, \dots, n_{\Pi}\}$ . In order to construct such a basis, we introduce the constraint matrix  $C^{(k)} : W^{(k)} \rightarrow \mathbb{R}^{n_{\Pi}^{(k)}}$  for each patch  $\Omega^{(k)}$  which realizes the primal variables, i. e.,  $(C^{(k)}v)_j = \psi_{i(k,j)}(v)$  for  $v \in W$  and  $j \in \{1, \dots, n_{\Pi}^{(k)}\}$ , where  $n_{\Pi}^{(k)}$  is the number of primal variables associated with  $\Omega^{(k)}$  and  $i(k, j)$  the global index of the  $j$ -th primal variable on  $\Omega^{(k)}$ . For each patch  $k$ , the basis functions  $\{\tilde{\phi}_j^{(k)}\}_{j=1}^{n_{\Pi}^{(k)}}$  of  $\tilde{W}_{\Pi}^{(k)}$  are the solution of the system

$$\begin{bmatrix} K_{BB}^{(k)} & K_{BI}^{(k)} & C^{(k)T} \\ K_{IB}^{(k)} & K_{II}^{(k)} & 0 \\ C^{(k)} & 0 & 0 \end{bmatrix} \begin{bmatrix} \tilde{\phi}_j^{(k)} \\ \cdot \\ \tilde{\mu}_j^{(k)} \end{bmatrix} = \begin{bmatrix} 0 \\ 0 \\ \mathbf{e}_j^{(k)} \end{bmatrix}, \quad (16)$$

158 where  $\mathbf{e}_j^{(k)} \in \mathbb{R}^{n_{\Pi}^{(k)}}$  is the  $j$ -th unit vector. Here we use an equivalent formulation with the  
159 system matrix  $K^{(k)}$  For each patch  $k$ , the LU factorization of this matrix is computed and  
160 stored.

*Application of  $S_{\Delta\Delta}^{(k)-1}$*  : . The application of  $S_{\Delta\Delta}^{(k)-1}$  corresponds to solving a local Neumann problem in the space  $\widetilde{W}_\Delta$ , i.e.,  $S^{(k)}w^{(k)} = f_\Delta^{(k)}$  with the constraint  $C^{(k)}w^{(k)} = 0$ . This problem can be rewritten as a saddle point problem in the form

$$\begin{bmatrix} K_{BB}^{(k)} & K_{BI}^{(k)} & C^{(k)T} \\ K_{IB}^{(k)} & K_{II}^{(k)} & 0 \\ C^{(k)} & 0 & 0 \end{bmatrix} \begin{bmatrix} w^{(k)} \\ \cdot \\ \cdot \end{bmatrix} = \begin{bmatrix} f_\Delta^{(k)} \\ 0 \\ 0 \end{bmatrix}.$$

161 From (16), the LU factorization of the matrix is already available.

*Application of  $\mathbf{S}_{\text{III}}^{(k)-1}$*  : . The matrix  $\mathbf{S}_{\text{III}}$  can be assembled from the patch local matrices  $\mathbf{S}_{\text{III}}^{(k)}$ . Let  $\{\tilde{\phi}_j^{(k)}\}_{j=1}^{n_\Pi^{(k)}}$  be the basis of  $\widetilde{W}_\Pi^{(k)}$ . The construction of  $\{\tilde{\phi}_j^{(k)}\}_{j=1}^{n_\Pi^{(k)}}$  in (16) provides

$$\begin{aligned} \left(\mathbf{S}_{\text{III}}^{(k)}\right)_{i,j} &= \left\langle S^{(k)}\tilde{\phi}_i^{(k)}, \tilde{\phi}_j^{(k)} \right\rangle = - \left\langle C^{(k)T}\tilde{\mu}_i^{(k)}, \tilde{\phi}_j^{(k)} \right\rangle = - \left\langle \tilde{\mu}_i^{(k)}, C^{(k)}\tilde{\phi}_j^{(k)} \right\rangle \\ &= - \left\langle \tilde{\mu}_i^{(k)}, \mathbf{e}_j \right\rangle^{(k)} = - \left(\tilde{\mu}_i^{(k)}\right)_j, \end{aligned}$$

162 where  $i, j \in \{1, \dots, n_\Pi^{(k)}\}$ . Therefore, we can reuse the Lagrange multipliers  $\tilde{\mu}_i^{(k)}$  obtained  
163 in (16), and can assemble  $\mathbf{S}_{\text{III}}^{(k)}$  from them. Once  $\mathbf{S}_{\text{III}}$  is assembled, the LU factorization  
164 can be calculated and stored.

#### 165 4.2.2. Application of $\tilde{I}$ and $\tilde{I}^T$

166 The last building block is the embedding  $\tilde{I} : \widetilde{W} \rightarrow W$  and its adjoint  $\tilde{I}^T : W^* \rightarrow \widetilde{W}^*$ .  
167 Recall the direct splitting  $W^{(k)} = W_\Delta^{(k)} \oplus W_\Pi^{(k)}$ . Let us denote by  $\Phi^{(k)} = [\tilde{\phi}_1^{(k)}, \dots, \tilde{\phi}_{n_\Pi^{(k)}}^{(k)}]$  the  
168 coefficient representation of the basis for  $W_\Pi^{(k)}$ . Given the primal part  $\mathbf{w}_\Pi$  of a function in  
169  $\widetilde{W}$ , we obtain its restriction to  $\widetilde{W}_\Pi^{(k)}$  via an appropriately defined restriction matrix  $\mathbf{R}^{(k)}$ ,  
170 i.e.  $\mathbf{w}_\Pi^{(k)} = \mathbf{R}^{(k)}\mathbf{w}_\Pi$ . The corresponding function is then given by  $w_\Pi^{(k)} = \Phi^{(k)}\mathbf{R}^{(k)}\mathbf{w}_\Pi^{(k)}$ .

Following the lines in [42], we can formulate the operator  $\tilde{I} : \widetilde{W} \rightarrow W$  as

$$\begin{bmatrix} \mathbf{w}_\Pi \\ w_\Delta \end{bmatrix} \mapsto w := \Phi \mathbf{R} \mathbf{w}_\Pi + w_\Delta,$$

where  $\Phi$  and  $\mathbf{R}$  are block versions of  $\Phi^{(k)}$  and  $\mathbf{R}^{(k)}$ , respectively. The second function is its adjoint operation  $\tilde{I}^T : W^* \rightarrow \widetilde{W}^*$ . It can be realized in the following way

$$f \mapsto \begin{bmatrix} \mathbf{f}_\Pi \\ f_\Delta \end{bmatrix} = \begin{bmatrix} \mathbf{A}\Phi^T \mathbf{f} \\ f - C^T \Phi^T \mathbf{f} \end{bmatrix},$$

171 where  $\mathbf{A}$  is the corresponding assembling operator to  $\mathbf{R}$ , i.e.,  $\mathbf{A} = \mathbf{R}^T$ . A more extensive  
172 discussion and derivation can be found in [42].

## 173 5. Parallelization of the building blocks

174 Here we investigate how the single operations can be executed in parallel in a distributed  
175 memory setting. The parallelization of the method is performed with respect to the

---

**Algorithm 1** Algorithm for calculating  $\boldsymbol{\nu} = F\boldsymbol{\lambda}$  and  $\boldsymbol{\nu} = M_{sD}^{-1}\boldsymbol{\lambda}$  for given  $\boldsymbol{\lambda} \in U$ 


---

```

procedure  $F(\boldsymbol{\lambda})$ 
  Application of  $B^T : \{f^{(k)}\}_{k=1}^N = B^T \boldsymbol{\lambda}$ 
  Application of  $\tilde{I}^T : \{\mathbf{f}_\Pi, \{f_\Delta^{(k)}\}_{k=1}^N\} = \tilde{I}^T (\{f^{(k)}\}_{k=1}^N)$ 
  Application of  $\tilde{S}^{-1} :$ 
  Begin
     $\mathbf{w}_\Pi = \mathbf{S}_{\Pi\Pi}^{-1} \mathbf{f}_\Pi$ 
     $w_\Delta^{(k)} = S_{\Delta\Delta}^{(k)-1} f_\Delta^{(k)} \quad \forall k = 1, \dots, N$ 
  End
  Application of  $\tilde{I} : \{w^{(k)}\}_{k=1}^N = \tilde{I} (\{\mathbf{w}_\Pi, \{w_\Delta^{(k)}\}_{k=1}^N\})$ 
  Application of  $B : \boldsymbol{\nu} = B (\{w^{(k)}\}_{k=1}^N)$ 
end procedure
procedure  $M_{sD}^{-1}(\boldsymbol{\lambda})$ 
  Application of  $B_D^T : \{w^{(k)}\}_{k=1}^N = B_D^T \boldsymbol{\lambda}$ 
  Application of  $S_e :$ 
  Begin
    Solve  $K_{II}^{(k)} x^{(k)} = -K_{IB}^{(k)} w^{(k)} \quad \forall k = 1, \dots, N$ 
     $v^{(k)} = K_{BB}^{(k)} w^{(k)} + K_{BI}^{(k)} x^{(k)}. \quad \forall k = 1, \dots, N$ 
  End
  Application of  $B_D : \boldsymbol{\nu} = B_D (\{v^{(k)}\}_{k=1}^N)$ 
end procedure

```

---

176 patches, i.e., one or several patches are assigned to a processor. The required communi-  
 177 cation has to be understood as communication between patches, which are assigned to  
 178 different processors. The majority of the used MPI methods are performed in its non-  
 179 blocking version. We aim at overlapping computations with communications wherever  
 180 possible.

### 181 5.1. Parallel version of PCG

182 We solve  $F\boldsymbol{\lambda} = d$  with the preconditioned CG method. This requires a parallel imple-  
 183 mentation of CG, where we follow the approach presented in Section 2.2.5.5 in [42], see  
 184 also [11]. This approach is based on the concept of accumulated and distributed vectors.  
 185 We say a vector  $\boldsymbol{\lambda}_{acc} = [\boldsymbol{\lambda}_{acc}^{(q)}]$  is an *accumulated* representation of  $\boldsymbol{\lambda}$ , if  $\boldsymbol{\lambda}_{acc}^{(q)}(k_q(i)) = \boldsymbol{\lambda}(i)$ ,  
 186 where  $i$  is the global index corresponding to the local index  $k_q(i)$  on processor  $q$ . On the  
 187 contrary,  $\boldsymbol{\lambda}_{dist} = [\boldsymbol{\lambda}_{dist}^{(q)}]$  is a *distributed* representation of  $\boldsymbol{\lambda}$ , if the sum of all processor  
 188 local contributions give the global vector, i.e.,  $\boldsymbol{\lambda}_{dist}(i) = \sum_q \boldsymbol{\lambda}_{dist}^{(q)}(k_q(i))$ . Hence, each  
 189 processor only holds the part of  $\boldsymbol{\lambda}$ , which belongs to its patches, either in a distributed or  
 190 accumulated description. The Lagrange multipliers and the search direction of the CG are  
 191 represented in the accumulated setting, whereas the residual is given in the distributed  
 192 representation. In order to achieve the accumulated representation, information exchange  
 193 between the neighbours of a patch is required. This is done after applying the matrix and  
 194 the preconditioner, respectively and implemented via MPI\_Send and MPI\_Recv operations.

195 The last aspect in the parallel CG implementation is the realization of scalar products.  
 196 Given a distributed representation  $u_{dist}$  of  $u$  and an accumulated representation of  $v_{acc}$  of

197  $v$ , the scalar product  $(u, v)_{l^2}$  is then given by  $(u, v)_{l^2} = \sum_q (u_{dist}^{(q)}, v_{acc}^{(q)})_{l^2}$ , i.e., first the local  
 198 scalar products are formed, globally added, and distributed with `MPI_Allreduce` .

### 199 5.2. Assembling

200 The assembling routine of the IETI-DP algorithm consists of the following steps:

- 201 1. Assemble the patch local stiffness matrices and right hand side,
- 202 2. assemble the system matrix in (16) and calculating its LU-factorization,
- 203 3. assemble  $S_{III}$  and calculating its LU-factorization,
- 204 4. calculate the LU-factorization of  $K_{II}^{(k)}$  ,
- 205 5. calculate the right hand side  $\{g_{II}, g_{\Delta}\} = \tilde{g} \in \widetilde{W}^*$ , with  $g^{(k)} = f_B - K_{BI}^{(k)}(K_{II}^{(k)})^{-1}f_I^{(k)}$ .

206 Most of the tasks are completely independent of each other and, hence, can be performed  
 207 in parallel. Only the calculation of  $S_{III}$  and  $\tilde{g} = \widetilde{I}^T g$  require communication, which will  
 208 be handled in Section 5.3.

209 The LU-factorization of  $S_{III}$  is only required at one processor, since it has to be solved  
 210 only once per CG iteration. According to [29], it is advantageous to distribute this matrix  
 211 to all other processors in order to reduce communication in the solver part, see [32] and  
 212 references therein for improving scalability based on a different approach. In the current  
 213 paper, we investigate cases, where one, several and all processor hold the LU-factorization  
 214 of  $S_{III}$ . Therefore, each processor is assigned to exactly one holder of  $S_{III}$ . This relation  
 215 is implemented by means of an additional MPI communicator.

216 We note that, for extremely large scale problems with  $\geq 10^5$  subdomains, one has to  
 217 consider different strategies dealing with  $S_{III}^{-1}$ . Most commonly one uses AMG and solves  
 218  $S_{III}u_{II} = f_{II}$  in an inexact way, see, e.g., [27] and [31]. When considering a moderate  
 219 number of patches, i.e.,  $10^3 - 10^4$ , the approach using the LU-factorization of  $S_{III}$  is the  
 220 most efficient one. In this paper, we restrict ourselves to this case.

221 The patch local matrix  $S_{III}^{(k)}$  is obtained as a part of the solutions of (16) and the assem-  
 222 bling of the global matrix  $S_{III}$  is basically a `MPI_gatherv` operation. In the case where  
 223 all processors hold  $S_{III}$  we use `MPI_allgatherv`. If several processors hold the LU fac-  
 224 torization, we just call `MPI_gatherv` on each of these processors. A different possibility  
 225 would be to first assemble  $S_{III}$  on one patch, distribute it to the other holders and then  
 226 calculate the LU-factorization on each of the processors.

### 227 5.3. Solver and Preconditioner

228 More communication is involved in the solver part. According to Algorithm 1, we have to  
 229 perform the following operations:

- 230 1. application of  $B$  and  $B^T$  and its scaled versions
- 231 2. application of  $\widetilde{I}$  and  $\widetilde{I}^T$
- 232 3. application of  $\widetilde{S}^{-1}$
- 233 4. application of  $S^{-1}$

234 The only operations which require communication are  $\widetilde{I}$  and  $\widetilde{I}^T$ . To be more precise,  
 235 the communication is hidden in the operators  $\mathbf{A}$  and  $\mathbf{R}$ , see Section 4.2, all other oper-  
 236 ations are block operations, where the corresponding matrices are stored locally on each

237 processor. In principle, their implementation is given by accumulating and distributing  
 238 values. The actual implementation depends on how many processors hold the coarse grid  
 239 problem.

240 In order to implement  $\tilde{I}$ , we need the distribution operation  $\mathbf{R}$ . If all processors hold  
 241  $S_{\text{III}}$ , this operations reduces to just extracting the right entries. Hence it is local and  
 242 no communication is required. Otherwise, each holder of  $S_{\text{III}}$  reorders and duplicates  
 243 the entries of  $\mathbf{w}_{\text{II}}$  in such a way, that all entries corresponding to the patches of a single  
 244 slave are in a contiguous block of memory. Then we utilize the `MPI_scatter` method to  
 245 distribute only the necessary data to all slave processors. See Figure 1 for an illustration.

246 We arrive at the implementation of  $\tilde{I}^T$ . Each processor stores the values of  $\mathbf{w}_{\text{II}}^{(k)}$  in a  
 247 vector  $\tilde{\mathbf{w}}_{\text{II}}^{(k)}$  of length  $n_{\text{II}}$  already in such a way, that  $\sum_{k=1}^N \tilde{\mathbf{w}}_{\text{II}}^{(k)} = \mathbf{w}_{\text{II}}$ . Storing the entries  
 248 in this way enables the use the MPI reduction operations to efficiently assemble the local  
 249 contributions. If only one processor holds the coarse problem, we use the `MPI_Reduce`  
 250 method to perform this operation. Similarly, if all processors hold  $S_{\text{III}}$ , we utilize the  
 251 `MPI_Allreduce` method. If several processors have the coarse grid problem, we use a  
 252 two level approach. First, each master processor collects the local contributions from  
 253 its slaves using the `MPI_Reduce` operation. In the second step, all the master processors  
 254 perform an `MPI_Allreduce` operation to accumulate the contributions from each group  
 255 and simultaneously distribute the result under them. This procedure is visualized in  
 256 Figure 1.

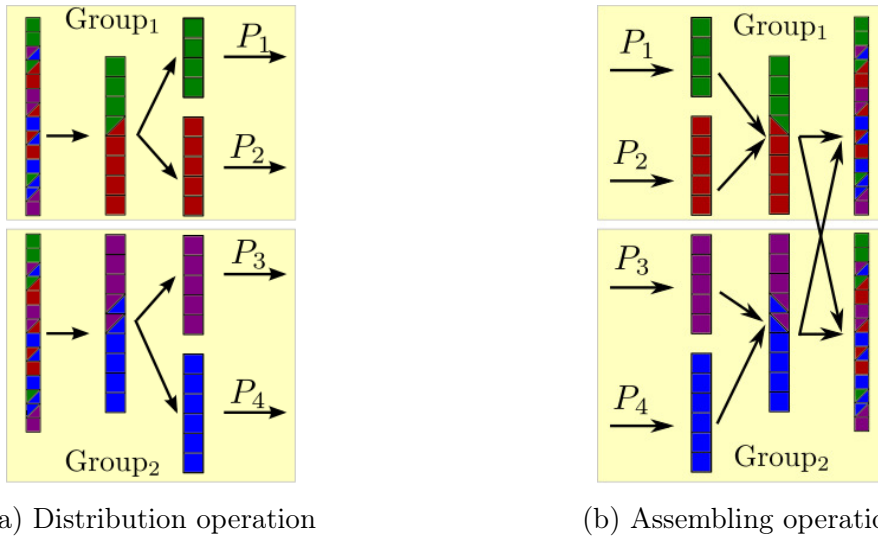


Figure 1: Distribution and assembling operation, illustrated for four processors, partitioned into two groups corresponding to two  $S_{\text{III}}^{-1}$  holder.

## 257 6. Numerical examples

258 We consider the model problem (1) in the two dimensional computational domain  $\Omega =$   
 259  $(0, 1)^2$  formed by  $32 \times 32 = 1024$  patches. Each of them is a square arranged in a  
 260 uniform grid. For the three dimensional case we consider the domain  $\Omega = (0, 1)^2 \times (0, 2)$ ,  
 261 partitioned into  $8 \times 8 \times 16$  regular cubes. Note that, in IgA framework, we cannot choose  
 262 the number of subdomains as freely as in the finite element case since they are fixed by  
 263 the geometry. Therefore, the number of 1024 subdomains stays constant throughout the

264 tests. Since we are interested in the parallel scalability of the proposed algorithms, we  
 265 assume for simplicity homogeneous diffusion coefficients  $\alpha \equiv 1$ . In all tests we consider the  
 266 smooth right hand side  $f(x, y) = 20\pi^2 \sin(4\pi(x + 0.4)) \sin(2\pi(y + 0.3))$ , corresponding to  
 267 the exact solution  $u(x, y) = \sin(4\pi(x + 0.4)) \sin(2\pi(y + 0.3)) + x + y$ . For the discretization,  
 268 we use tensor B-Spline spaces  $V_h$  of different degree  $p$ . We increase the B-Spline degree in  
 269 such a way that the number of knots stay the same, i.e., the smoothness of  $V_h$  increases.

270 We investigate the scaling behaviour of the cG-IETI-DP and dG-IETI-DP method. Al-  
 271 though, we consider also the dG variant, we restrict ourselves to matching meshes. Oth-  
 272 erwise, it would not be possible to compare the two methods. Moreover, some patches  
 273 would have a significant larger number of dofs, which leads to load imbalances and affects  
 274 the scaling in a negative way. The domain is refined in a uniform way by inserting a  
 275 single knot for each dimension on each knot span. We denote by  $H_k$  the patch diameter  
 276 and by  $h_k$  the characteristic mesh size on  $\Omega^{(k)}$ . The set of primal variables is chosen by  
 277 continuous patch vertices and interface averages for the two dimensional setting. For the  
 278 three dimensional examples, we choose only continuous edge averages in order to keep the  
 279 number of primal variables small.

280 The preconditioned conjugate gradient method is used to solve (14) with the scaled Dirich-  
 281 let preconditioner  $M_{sD}^{-1}$ . We choose zero initial guess and a relative reduction of the resid-  
 282 ual of  $10^{-8}$ . For solving the local systems and the coarse grid problem, a direct solver is  
 283 used.

284 The algorithm is realized in the isogeometric open source C++ library G+SMO [40],  
 285 which is based on the Eigen library [17]. We utilize the PARDISO 5.0.0 Solver Project  
 286 [35] for performing the LU factorizations. The code is compiled with the gcc 4.8.3  
 287 compiler with optimization flag `-O3`. For the communication between the processors, we  
 288 use the MPI 2 standard with the OpenMPI 1.10.2 implementation. The results are obtain  
 289 on the RADON1 cluster at Linz. We use 64 out of 68 available nodes, each equipped with  
 290 2x Xeon E5-2630v3 ‘‘Haswell’’ CPU (8 Cores, 2.4Ghz, 20MB Cache) and 128 GB RAM.  
 291 This gives the total number of 1024 available cores.

292 We investigate two quantities, the assembling phase and the solving phase. In the assem-  
 293 bling phase, we account for the time used for

- 294 • assembling the local matrices and right hand sides,
- 295 • LU-factorization of  $K_{II}$ ,
- 296 • LU-factorization of  $\begin{bmatrix} K & C^T \\ C & 0 \end{bmatrix}$ ,
- 297 • calculation of  $\tilde{\Phi}$  and  $\tilde{\mu}$ ,
- 298 • assembling the coarse grid matrix  $S_{III}$  and calculation of its LU factorization.

299 As already indicated in Section 5,  $S_{III}$  is only assembled on certain processors. The  
 300 solving phase consists of the CG algorithm for (14) and the back-substitution to obtain  
 301 the solution from the Lagrange multipliers. The main ingredients are

- 302 • application of  $F$ ,
- 303 • application of  $M_{sD}^{-1}$ .

304 In Section 6.1 and Section 6.2, we study the weak and strong scaling behaviour for the  
 305 cG-IETI-DP and the dG-IETI-DP method. In this two sections, we assume that only one  
 306 processor holds the coarse grid matrix  $S_{\text{III}}$ . The comparison of having a different number  
 307 of  $S_{\text{III}}$  holders is done in Section 6.3.

### 308 6.1. Weak scaling

309 In this subsection we investigate the weak scaling behaviour, i.e., the relation of problem  
 310 size and number of processors is constant. In each refinement step we multiply the number  
 311 of used cores by  $2^d$ ,  $d \in \{2, 3\}$ . The ideal behaviour would be a constant time for each  
 312 refinement.

313 First, we consider the two dimensional case. We apply three initial refinements and start  
 314 with a single processor and perform up to additional 5 refinements with maximum 1024  
 315 processors. We choose as primal variables continuous vertex values and edge averages.  
 316 The results for degree  $p \in \{2, 3, 4\}$  are illustrated in Figure 2. The first row of figures  
 317 corresponds to the cG-IETI-DP method, and the second one corresponds to the dG-  
 318 IETI-DP method. The left column of Table 1 summarizes timings and the speedup for  
 319 the cG-IETI-DP method, whereas the right column presents the results for the dG-IETI-  
 320 DP method. For each method, we investigate the weak scaling for the assembling and  
 321 solution phase. As in Figure 2, we present the scaling and timings for  $p \in \{2, 3, 4\}$ .

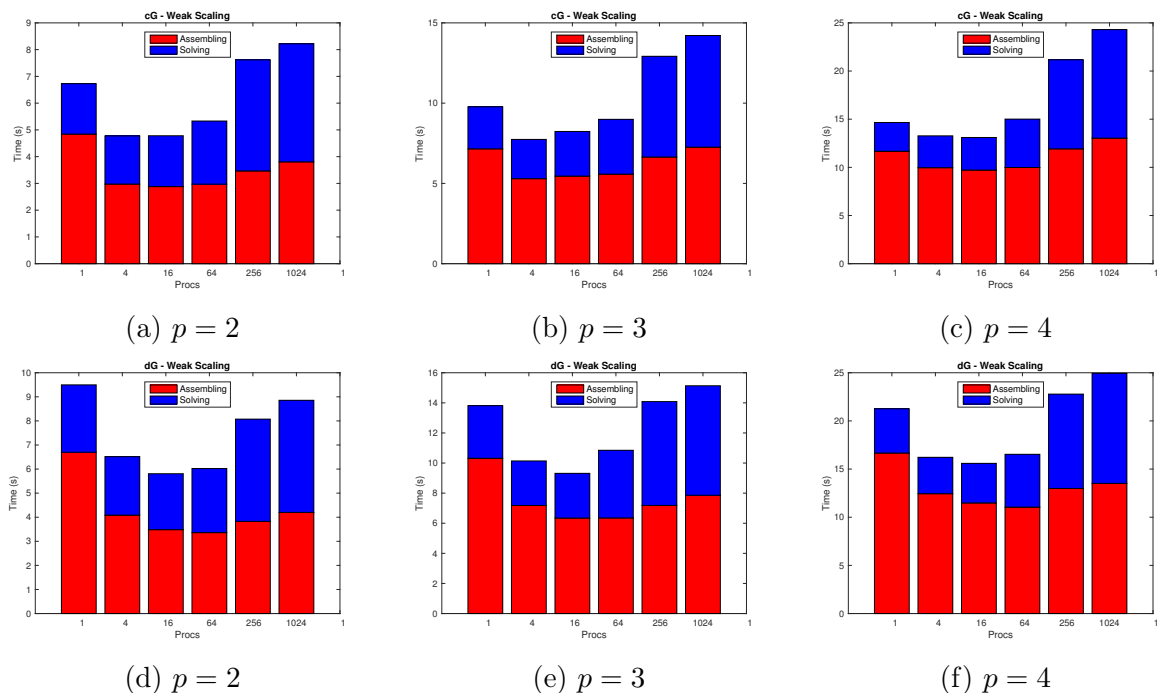


Figure 2: Weak scaling of the cG-IETI-DP (first row) and dG-IETI-DP (second row) method for B-Spline degrees  $p \in \{2, 3, 4\}$  in two dimensions. Each degree corresponds to one column.

322 We observe that the time used for the assembling stays almost constant, hence shows  
 323 quite optimal behaviour. However, the time for solving the system increases when re-  
 324 fining and increasing the number of used processors. Especially, when considering the  
 325 largest number of processors, we see a clear increase of the solution time. One reason is  
 326 that the number of iterations slightly increases when increasing the system size. This is  
 327 due to the quasi optimal condition number bound of the IETI-DP type methods, cf. (15).

cG-IETI-DP			$p = 2$			dG-IETI-DP			$p = 2$		
# procs	#dofs	Iter.	Ass. Time	Solv. Time	Total Time	#dofs	Iter.	Ass. Time	Solv. Time	Total Time	
1	99104	7	4.8	1.9	6.7	133824	8	6.7	2.8	9.5	
4	328224	8	3.0	1.8	4.8	394688	9	4.1	2.4	6.5	
16	1179680	9	2.9	1.9	4.8	1309632	10	3.5	2.3	5.8	
64	4455456	10	3.0	2.4	5.4	4712384	11	3.4	2.7	6.1	
256	17298464	11	3.5	4.2	7.7	17809344	11	3.8	4.2	8.0	
1024	68150304	11	3.8	4.4	8.2	69169088	12	4.2	4.7	8.9	
cG-IETI-DP			$p = 3$			dG-IETI-DP			$p = 3$		
# procs	#dofs	Iter.	Ass. Time	Solv. Time	Total Time	#dofs	Iter.	Ass. Time	Solv. Time	Total Time	
1	120576	8	7.2	2.6	9.8	159264	8	10.3	3.5	13.8	
4	366080	9	5.3	2.4	7.7	436512	9	7.2	3.0	10.2	
16	1250304	10	5.5	2.8	8.3	1384224	10	6.3	3.0	9.3	
64	4591616	10	5.6	3.4	9.0	4852512	11	6.4	4.5	10.9	
256	17565696	11	6.6	6.3	12.9	18080544	12	7.2	6.9	14.1	
1024	68679680	12	7.3	7.0	14.3	69702432	12	7.9	7.3	15.2	
cG-IETI-DP			$p = 4$			dG-IETI-DP			$p = 4$		
# procs	#dofs	Iter.	Ass. Time	Solv. Time	Total Time	#dofs	Iter.	Ass. Time	Solv. Time	Total Time	
1	144096	8	11.7	3.0	14.7	186752	9	16.7	4.6	21.3	
4	405984	9	10.0	3.3	13.3	480384	10	12.4	3.8	16.2	
16	1322976	10	9.7	3.4	13.1	1460864	11	11.5	4.1	15.6	
64	4729824	11	10.0	5.0	15.0	4994688	11	11.0	5.5	16.5	
256	17834976	12	11.9	9.3	21.2	18353792	12	13.0	9.8	22.8	
1024	69211104	13	13.0	11.3	24.3	70237824	13	13.5	11.4	24.9	

Table 1: Weak scaling results for the two dimensional testcase for the cG and dG IETI-DP method. Left column contains results for the cG variant and the right column for the dG version. Each row corresponds to a fixed B-Spline degree  $p \in \{2, 3, 4\}$

328 Secondly, as already pointed out in Section 5, the solving phase consists of more commu-  
329 nication between processors, which cannot be completely overlapped with computations.  
330 Moreover, one also has to take in account global synchronization points in the conjugate  
331 gradient method.

332 Next, we consider the weak scaling for the three dimensional case. As already indicated  
333 in the introduction of this section, we choose only continuous edge averages as primal  
334 variables. We perform the tests in the same way as for the two dimensional case. However,  
335 we already start with two processors and perform two initial refinements. Multiplying  
336 the number of used processors by 8 with each refinement, we end up again with 1024  
337 processors on the finest grid. The two algorithms behave similar to the two dimensional  
338 case, where the assembling phase gives quite good results and the solver phase shows  
339 again an increasing time after each refinement. The results are visualized in Figure 3 and  
340 summarized in Table 2. Note, for the dG-IETI-DP method with  $p = 4$  and  $\sim 54$  Mio.  
341 dofs, we exceeded the memory capacity of the cluster.

## 342 6.2. Strong scaling

343 Secondly, we are investigating the strong scaling behaviour. Now we fix the problem size  
344 and increase the number of processors. In the optimal case, the time used by a certain  
345 quantity reduces in the same way as the number of used processors increases. We use

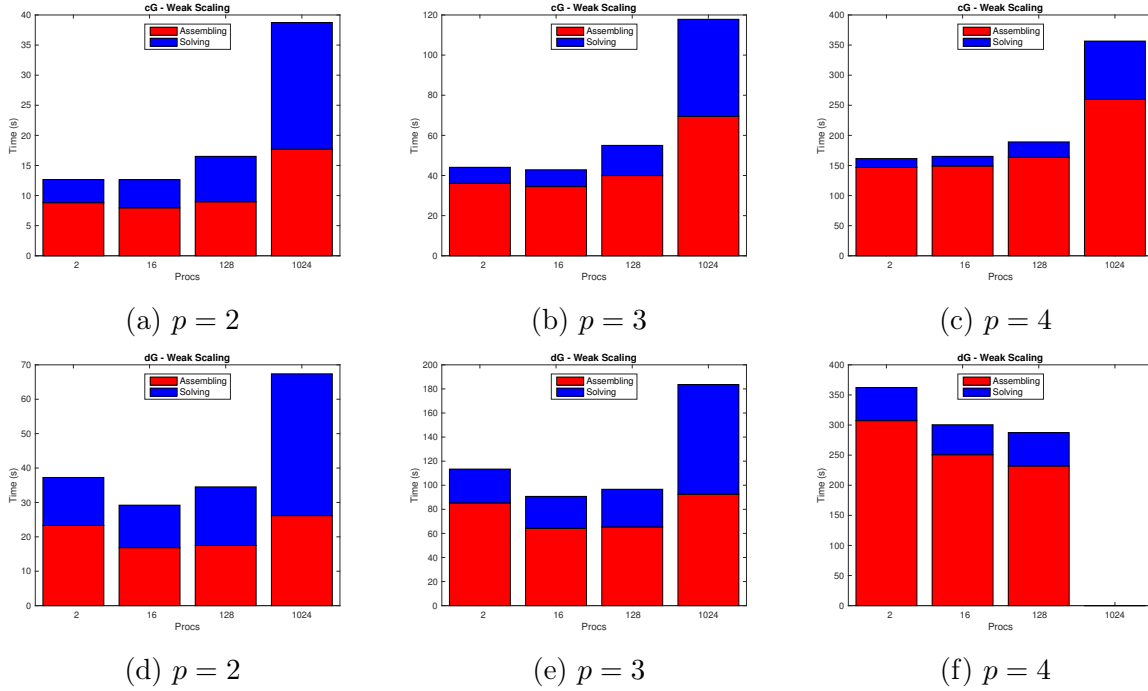


Figure 3: Weak scaling of the cG-IETI-DP (first row) and dG-IETI-DP (second row) method for B-Spline degrees  $p \in \{2, 3, 4\}$  in three dimensions. Each degree corresponds to one column. No timings are obtained in the case of 1024 cores in (f) due to memory limitations

346 the same primal variables for the strong scaling studies as in the weak scaling studies in  
 347 Section 6.1.

348 Again as in Section 6.1, we begin with the two dimensional example. We perform 7 initials  
 349 refinements and end up with 17 Mio. dofs on 1024 subdomains. We start already with  
 350 4 processors in the initial case and do 8 refinements until we reach 1024 cores. Similar  
 351 to Section 6.1, the results for  $p \in \{2, 3, 4\}$  are illustrated in Figure 4 and summarized in  
 352 Table 3.

353 We observe that the assembling phase has a quite good scaling performance, as already  
 354 observed for the weak scaling results in Section 6.1. Moreover, the higher the B-Spline  
 355 degree, the better the parallel performance behaves. This holds due to increased computa-  
 356 tional costs for the parallel part. Similar to the weak scaling results, the solver phase does  
 357 not provide such an excellent scaling as the assembling phase. Still, we obtain a scaling  
 358 from around 500 when using 1024 processors. We note that the degree of the B-Splines  
 359 does not seem to have such a significant effect on the scaling for the solver phase as for  
 360 the assembling phase.

361 In the three dimensional example we perform four initial refinements and obtain around  
 362 5 Mio. dofs. The presentation of the results is done in the same way as in the previous  
 363 examples, see Figure 5 and Table 4. Also in three dimensions the cG-IETI-DP algorithms  
 364 behaves very similarly to the two dimensional case, showing excellent scaling results.  
 365 However, the dG version of the algorithm shows a good scaling but not as promising as  
 366 cG version. Especially, when considering  $p = 2$ , we observe degraded scalability for the  
 367 assembling phase. Having a closer look at the timings, we observe that this originates  
 368 from small load imbalances in the interior domains, due to the additional layer of dofs  
 369 and the larger number of primal variables. The latter one leads to an increased time in

cG-IETI-DP			$p = 2$			dG-IETI-DP			$p = 2$		
# procs	#dofs	Iter.	Ass. Time	Solv. Time	Total Time	#dofs	Iter.	Ass. Time	Solv. Time	Total Time	
2	220896	16	8.8	3.8	12.6	396932	26	23.3	14.0	37.3	
16	1023200	17	8.0	4.7	12.7	1551400	27	16.9	12.3	29.2	
128	5969376	17	9.0	7.5	16.5	7730288	28	17.5	17.0	34.5	
1024	40238048	19	17.7	21.0	38.7	46577920	28	26.2	41.2	67.4	
cG-IETI-DP			$p = 3$			dG-IETI-DP			$p = 3$		
# procs	#dofs	Iter.	Ass. Time	Solv. Time	Total Time	#dofs	Iter.	Ass. Time	Solv. Time	Total Time	
2	350840	17	36.2	7.9	44.1	598405	29	85.3	28.1	113.4	
16	1361976	18	34.5	8.4	42.9	2005737	30	64.2	26.5	90.7	
128	7020728	18	40.0	15.0	55.0	8985265	30	65.4	31.3	96.7	
1024	43894200	21	69.4	48.4	117.8	50613825	31	92.6	91.0	183.6	
cG-IETI-DP			$p = 4$			dG-IETI-DP			$p = 4$		
# procs	#dofs	Iter.	Ass. Time	Solv. Time	Total Time	#dofs	Iter.	Ass. Time	Solv. Time	Total Time	
2	523776	18	146.6	14.8	161.4	853878	32	307.3	55.1	362.4	
16	1768320	18	149.2	15.9	165.1	2538650	32	250.7	49.8	300.5	
128	8188800	20	163.6	25.6	189.2	10367970	34	232.0	55.4	287.4	
1024	47765376	22	259.7	96.9	356.6	~54000000	x	x	x	x	

Table 2: Weak scaling results for the three dimensional testcase for the cG and dG IETI-DP method. Left column contains results for the cG variant and the right column for the dG version. Each row corresponds to a fixed B-Spline degree  $p \in \{2, 3, 4\}$ . No timings are available for the dG-IETI-DP method with  $p = 4$  on 1024 cores due to memory limitations.

370 solving (16), due to a larger number of right hand sides on the interior subdomains. One  
371 can further optimize the three dimensional case, by considering different strategies for  
372 the primal variables, where one aims for smaller and more equally distributed numbers of  
373 primal variables.

### 374 6.3. Study on the number of $S_{\text{III}}^{-1}$ holders

375 In this last section of the numerical experiments, we want to investigate the influence of  
376 the number of holders of  $S_{\text{III}}^{-1}$  on the scaling behaviour. As already indicated in Section 5.3,  
377 if more processors hold the LU-factorization of the coarse grid matrix, it is possible to  
378 decrease the communication effort after applying  $S_{\text{III}}^{-1}$ , while having more communication  
379 before the application. The advantage of this strategy is to be able to have a better  
380 overlap of communication with computations. However one has to take into account, that  
381 this also increases the communication in the assembling phase, since the local contribution  
382  $S_{\text{III}}^{(k)}$  has to be sent to all the master processors.

383 We only consider the two dimensional domain, where we perform 7 initials refinements,  
384 but on a decomposition with 4096 subdomains and end up with around 70 Mio. dofs.  
385 This gives a comparable setting as in Section 6.1 having the most refined domain. In order  
386 to better observe the influence of the number of  $S_{\text{III}}^{-1}$  holders, we increase the number of  
387 subdomains, leading to a larger coarse grid problem. We only investigate the case of using  
388 1024 processors and the number of  $S_{\text{III}}$  holders given by  $2^n, n \in \{0, 1, \dots, 10\}$ . Hence, we  
389 obtain the number of master processors ranging from 1 to 1024, such that each master  
390 has the same number of slaves. The results are summarized in Figure 6 and Table 5.

391 We observe that choosing several holders of the coarse grid problem in the cG version

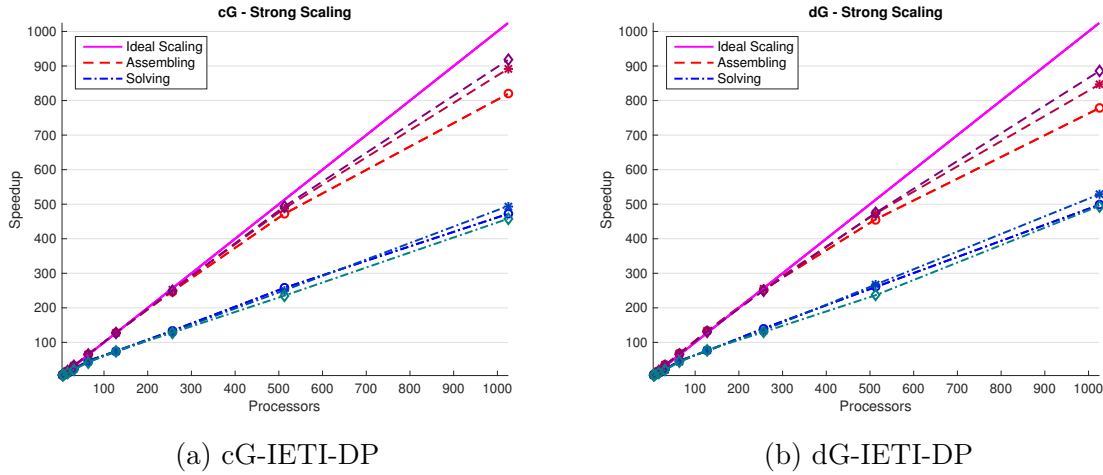


Figure 4: Strong scaling of the cG-IETI-DP (left column) and dG-IETI-DP (right column) method for B-Spline degrees  $p \in \{2, 3, 4\}$  in two dimensions. The markers  $\{\circ, *, \diamond\}$  as well as different shades of red (assembling phase) and blue (solver phase) correspond to the degrees  $\{2, 3, 4\}$ .

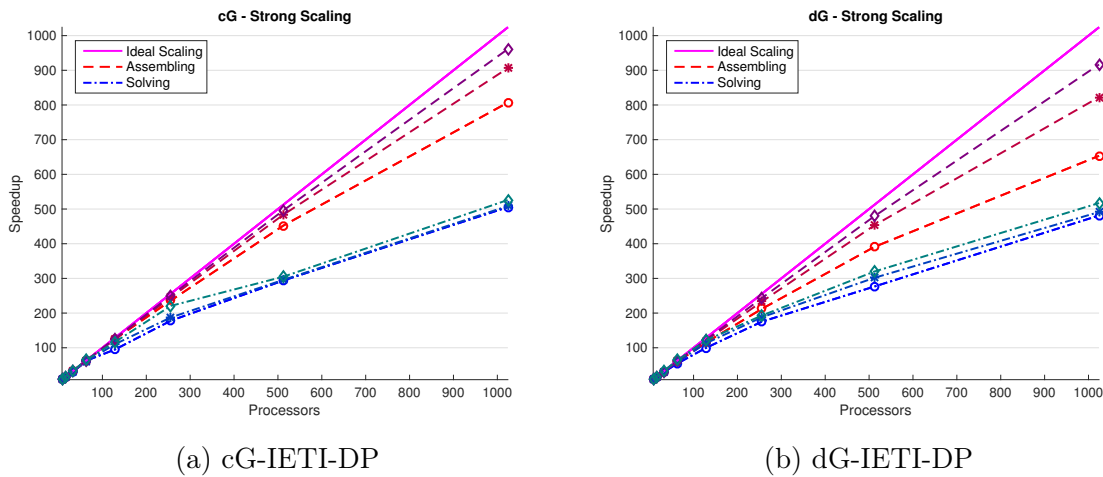


Figure 5: Strong scaling of the cG-IETI-DP (left column) and dG-IETI-DP (right column) method for B-Spline degrees  $p \in \{2, 3, 4\}$  in three dimensions. The markers  $\{\circ, *, \diamond\}$  as well as different shades of red (assembling phase) and blue (solver phase) correspond to the degrees  $\{2, 3, 4\}$ .

392 does not really have a significant effect. However, in the dG version, due to an increased  
 393 number of primal variables, the use of several holders actually increases the performance  
 394 of the solver by around 10%. Nevertheless, what is gained in the solving part does not pay  
 395 off with the additional effort in the assembling phase. Considering the total computation  
 396 time in Table 5, the best options is still either using only a single coarse grid problem on  
 397 one processor or making a redundant factorization on each processor.

## 398 7. Conclusion

399 We have investigated the parallel scalability of the cG-IETI-DP and dG-IETI-DP method,  
 400 respectively. Numerical tests showed a very good scalability in the strong and weak scal-  
 401 ing for the assembling phase for both methods. We reached a speedup of approximately  
 402 900 when using 1024 cores. Although the speedup of the solver phase is not as good as the  
 403 one for the assembler phase, we still reached a speedup of around 500 when using 1024

2d	$p = 2$				$p = 3$				$p = 4$			
	assembling phase		solving phase		assembling phase		solving phase		assembling phase		solving phase	
# procs	Time	Sp.	Time	Sp.	Time	Sp.	Time	Sp.	Time	Sp.	Time	Sp.
4	190.8	4	138.2	4	364.5	4	202.6	4	653.7	4	279.1	4
8	94.8	8	88.8	6	181.2	8	141.8	6	325.9	8	202.7	6
16	47.1	16	45.9	12	89.9	16	71.9	11	162.3	16	102.6	11
32	23.1	32	22.9	24	44.5	32	35.7	23	80.4	32	51.3	22
64	11.6	65	11.8	46	22.4	65	18.5	44	40.2	64	26.3	42
128	5.9	127	7.3	75	11.3	128	11.1	73	20.4	128	14.8	75
256	3.0	247	4.1	133	5.7	251	6.1	131	10.4	250	8.7	128
512	1.6	471	2.1	257	2.9	487	3.2	250	5.3	493	4.7	235
1024	0.9	819	1.1	472	1.6	891	1.6	494	2.8	917	2.4	456

dG-IETI-DP	assembling phase		solving phase		assembling phase		solving phase		assembling phase		solving phase	
	Time	Sp.	Time	Sp.	Time	Sp.	Time	Sp.	Time	Sp.	Time	Sp.
4	216.6	4	144.0	4	402.2	4	225.5	4	711.8	4	294.2	4
8	106.9	8	92.9	6	199.5	8	156.8	5	352.6	8	210.6	5
16	52.5	16	47.9	12	98.1	16	80.4	11	174.3	16	106.4	11
32	25.1	34	25.7	22	47.5	33	42.2	21	84.9	33	55.2	21
64	12.7	68	12.2	47	23.9	67	20.4	44	42.9	66	27.0	43
128	6.5	132	7.6	75	12.0	134	11.6	77	21.7	131	15.1	77
256	3.4	252	4.1	140	6.2	255	6.6	135	11.4	249	9.0	129
512	1.9	455	2.2	260	3.4	472	3.3	267	6.0	474	4.9	236
1024	1.1	777	1.1	498	1.9	846	1.7	528	3.2	885	2.3	494

Table 3: Strong scaling results: Time (s) and Speedup for  $p \in \{2, 3, 4\}$  in two dimensions having approximately 17 Mio. dofs. First row shows results for the cG variant of the IETI-DP method, whereas the second row contains results for the dG version. Each column corresponds to a degree  $p$ .

404 cores. One can even increase the parallel performance of the solver part by increasing  
405 the number of processors, which are holding the coarse grid problem. However, numer-  
406 ical examples have shown that this does not really pay off in the total time, due to an  
407 increased assembling time. To summarize, we saw that the proposed methods are well  
408 suited for large scale parallelization of assembling and solving IgA equations in two and  
409 three dimensions.

## 410 Acknowledgements

411 This work was supported by the Austrian Science Fund (FWF) under the grant W1214-  
412 N15, project DK4. This support is gratefully acknowledged. Moreover, the author wants  
413 to thank Prof. Ulrich Langer for the valuable comments and support during the prepara-  
414 tion of the paper. He also gratefully acknowledges the support of Katharina Rafetseder  
415 of the Institute of Numerical Mathematics, Johannes Kepler University Linz (JKU) and  
416 Ioannis Touloupoulos and Angelos Mantzafaris, Radon Institute of Computational and  
417 Applied Mathematics Linz (RICAM).

## 418 References

- 419 [1] Y. Bazilevs, L. Beirão da Veiga, J. A. Cottrell, T. J. R. Hughes, and G. Sangalli.  
420 Isogeometric analysis: Approximation, stability and error estimates for  $h$ -refined  
421 meshes. *Math. Models Methods Appl. Sci.*, 16(7):1031–1090, 2006.

3d	$p = 2$				$p = 3$				$p = 4$			
	assembling phase		solving phase		assembling phase		solving phase		assembling phase		solving phase	
# procs	Time	Sp.	Time	Sp.	Time	Sp.	Time	Sp.	Time	Sp.	Time	Sp.
8	140.4	8	93.7	8	624.8	8	205.3	8	2565.7	8	382.6	8
16	70.5	16	47.7	16	312.8	16	103.4	16	1285.6	16	182.5	17
32	35.2	32	25.0	30	157.0	32	53.7	31	643.3	32	93.7	33
64	17.5	64	11.9	63	78.6	64	27.2	60	322.5	64	46.6	66
128	9.0	125	7.9	95	40.2	124	14.9	110	163.0	126	26.4	116
256	4.8	236	4.2	178	20.4	245	8.8	187	82.1	250	13.9	221
512	2.5	452	2.6	294	10.3	483	5.6	296	41.4	496	10.0	305
1024	1.4	807	1.5	506	5.5	906	3.2	509	21.4	961	5.8	526

dG-IETI-DP	assembling phase		solving phase		assembling phase		solving phase		assembling phase		solving phase	
	Time	Sp.	Time	Sp.	Time	Sp.	Time	Sp.	Time	Sp.	Time	Sp.
8	249.6	8	210.8	8	985.8	8	433.2	8	3588.1	8	854.8	8
16	126.2	16	106.6	16	498.6	16	217.1	16	1792.9	16	405.7	17
32	65.0	31	56.6	30	255.4	31	110.3	31	913.5	31	205.0	33
64	33.1	60	30.5	55	128.5	61	58.2	60	460.0	62	105.9	65
128	17.4	115	17.0	99	65.5	120	30.7	113	234.3	123	56.4	121
256	9.4	212	9.6	175	33.8	233	18.4	188	117.8	244	35.4	193
512	5.1	391	6.1	277	17.4	453	11.5	302	59.9	479	21.4	320
1024	3.1	653	3.5	481	9.6	822	7.1	491	31.3	917	13.2	517

Table 4: Strong scaling results: Time (s) and Speedup for  $p \in \{2, 3, 4\}$  in three dimensions having approximately 5 Mio. dofs. First row shows results for the cG variant of the IETI-DP method, whereas the second row contains results for the dG version. Each column corresponds to a degree  $p$ .

- 422 [2] Y. Bazilevs, V. Calo, J. Cottrell, J. Evans, T. Hughes, S. Lipton, M. Scott, and  
423 T. Sederberg. Isogeometric analysis using T-splines. *Computer Methods in Applied  
424 Mechanics and Engineering*, 199(5–8):229 – 263, 2010. Computational Geometry and  
425 Analysis.
- 426 [3] L. Beirão da Veiga, A. Buffa, G. Sangalli, and R. Vázquez. Mathematical analysis  
427 of variational isogeometric methods. *Acta Numerica*, 23:157–287, 2014.
- 428 [4] L. Beirão da Veiga, D. Cho, L. F. Pavarino, and S. Scacchi. Overlapping Schwarz  
429 methods for isogeometric analysis. *SIAM J. Numer. Anal.*, 50(3):1394–1416, 2012.
- 430 [5] L. Beirão Da Veiga, D. Cho, L. F. Pavarino, and S. Scacchi. BDDC preconditioners  
431 for isogeometric analysis. *Math. Models Methods Appl. Sci.*, 23(6):1099–1142, 2013.
- 432 [6] L. Beirão da Veiga, D. Cho, L. F. Pavarino, and S. Scacchi. Isogeometric Schwarz  
433 preconditioners for linear elasticity systems. *Comput. Methods Appl. Mech. Eng.*,  
434 253:439–454, 2013.
- 435 [7] J. A. Cottrell, T. J. R. Hughes, and Y. Bazilevs. *Isogeometric Analysis, Toward  
436 Integration of CAD and FEA*. John Wiley and Sons, 2009.
- 437 [8] D. A. Di Pietro and A. Ern. *Mathematical aspects of discontinuous Galerkin methods*.  
438 Berlin: Springer, 2012.
- 439 [9] C. R. Dohrmann. A preconditioner for substructuring based on constrained energy  
440 minimization. *SIAM J. Sci. Comput.*, 25(1):246–258, 2003.

cG-IETI-DP	$p = 2$			$p = 3$			$p = 4$		
# $S_{\text{III}}^{-1}$ Holder	Assemble Time	Solving Time	Total Time	Assemble Time	Solving Time	Total Time	Assemble Time	Solving Time	Total Time
1	3.61	3.66	7.27	6.50	5.52	12.02	11.23	8.30	19.53
2	4.49	3.58	8.07	7.97	5.57	13.54	13.83	8.02	21.85
4	4.53	3.82	8.35	7.65	5.40	13.05	13.60	8.09	21.69
8	4.46	3.63	8.09	7.72	5.76	13.48	13.32	8.15	21.47
16	4.34	3.49	7.83	7.64	5.61	13.25	13.16	7.93	21.09
32	4.33	3.73	8.06	7.74	5.39	13.13	13.15	8.78	21.93
64	4.34	3.59	7.93	7.62	5.45	13.07	13.10	8.04	21.14
128	4.49	4.06	8.55	7.60	6.05	13.65	13.06	8.47	21.53
256	4.31	4.64	8.95	7.63	6.43	14.06	13.02	8.81	21.83
512	4.34	3.61	7.95	7.55	5.71	13.26	13.23	8.09	21.32
1024	3.73	3.80	7.53	6.56	5.77	12.33	11.19	8.26	19.45

dG-IETI-DP	$p = 2$			$p = 3$			$p = 4$		
# $S_{\text{III}}^{-1}$ Holder	Assemble Time	Solving Time	Total Time	Assemble Time	Solving Time	Total Time	Assemble Time	Solving Time	Total Time
1	4.57	5.09	9.66	7.28	7.16	14.44	12.44	10.01	22.45
2	5.23	4.16	9.39	9.10	6.26	15.36	15.02	9.01	24.03
4	5.25	4.18	9.43	9.12	6.58	15.70	14.93	8.73	23.66
8	5.19	4.28	9.47	8.97	6.29	15.26	14.95	9.30	24.25
16	5.26	4.20	9.46	8.78	6.41	15.19	14.79	9.16	23.95
32	5.11	4.64	9.75	8.82	6.29	15.11	14.96	9.05	24.01
64	5.35	4.75	10.1	9.06	6.87	15.93	14.85	9.37	24.22
128	5.07	6.06	11.13	8.88	8.25	17.13	14.61	10.65	25.26
256	5.07	5.89	10.96	8.66	7.77	16.43	14.52	11.32	25.84
512	5.03	6.15	11.18	8.66	8.29	16.95	14.43	11.16	25.59
1024	4.70	5.33	10.03	7.45	7.68	15.13	12.89	10.60	23.49

Table 5: Influence of the number of processors having an LU-factorization of  $S_{\text{III}}$ . Timings in seconds for 1024 Processors on a domain with around 70 Mio. dofs and 2048 subdomains.

- 441 [10] C. R. Dohrmann. An approximate BDDC preconditioner. *Numerical Linear Algebra*  
442 *with Applications*, 14(2):149–168, 2007.
- 443 [11] C. C. Douglas, G. Haase, and U. Langer. *Tutorial on Elliptic PDE Solvers and Their*  
444 *Parallelization*. Society for Industrial and Applied Mathematics, Philadelphia, PA,  
445 USA, 2003.
- 446 [12] M. Dryja, J. Galvis, and M. Sarkis. BDDC methods for discontinuous Galerkin  
447 discretization of elliptic problems. *J. Complexity*, 23(4-6):715–739, 2007.
- 448 [13] M. Dryja, J. Galvis, and M. Sarkis. A FETI-DP preconditioner for a composite finite  
449 element and discontinuous Galerkin method. *SIAM J. Numer. Anal.*, 51(1):400–422,  
450 2013.
- 451 [14] M. Dryja and M. Sarkis. 3-d feti-dp preconditioners for composite finite element-  
452 discontinuous galerkin methods. In *Domain Decomposition Methods in Science and*  
453 *Engineering XXI*, pages 127–140. Springer, 2014.
- 454 [15] C. Giannelli, B. Jüttler, and H. Speleers. THB-splines: the truncated basis for  
455 hierarchical splines. *Comput. Aided Geom. Design*, 29, 2012.
- 456 [16] C. Giannelli, B. Jüttler, and H. Speleers. Strongly stable bases for adaptively refined  
457 multilevel spline spaces. *Advances in Computational Mathematics*, 40:459–490, 2014.

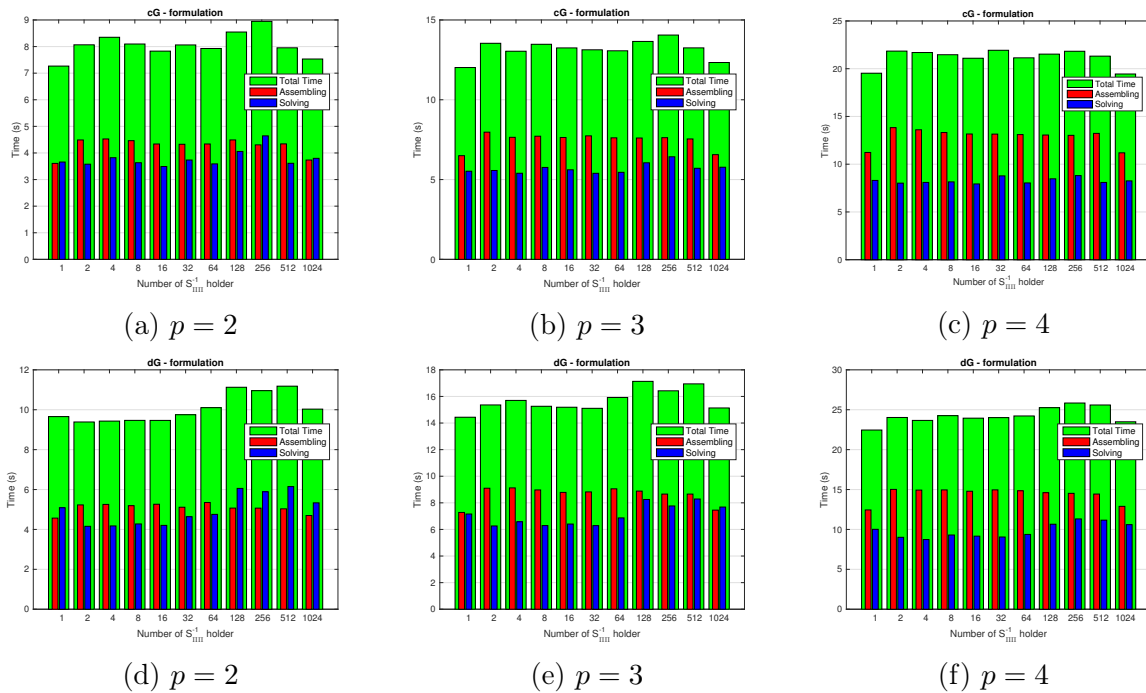


Figure 6: Influence of the number of  $S_{\text{III}}^{-1}$  holders on the scaling. First row corresponds to cG-IETI-DP, second row to dG-IETI-DP. Each column has a fixed degree  $p \in \{2, 3, 4\}$ . Figures (a-c) summarizes the cG version and Figures (d-f) the dG version, respectively.

- 458 [17] G. Guennebaud, B. Jacob, et al. Eigen v3. <http://eigen.tuxfamily.org>, 2010.
- 459 [18] C. Hofer and U. Langer. Dual-primal isogeometric tearing and interconnecting meth-  
460 ods. In P. Neittanmakki, J. Periaux, and O. Pironneau, editors, *Contributions to*  
461 *PDE for Applications*, Springer-ECCOMAS series "Computational Methods in Ap-  
462 *plied Sciences*". Springer, Berlin, Heidelberg, New York, 2016. to appear.
- 463 [19] C. Hofer and U. Langer. Dual-primal isogeometric tearing and intercon-  
464 necting solvers for multipatch dG-IgA equations. *Computer Methods in Ap-*  
465 *plied Mechanics and Engineering*, 2016. In Press, Accepted Manuscript,  
466 <http://dx.doi.org/10.1016/j.cma.2016.03.031>.
- 467 [20] C. Hofer, U. Langer, and I. Touloupoulos. Discontinuous Galerkin Isogeometric Anal-  
468 ysis of Elliptic Diffusion Problems on Segmentations with Gaps. *SIAM J. Sci. Com-*  
469 *put.*, 2016. Accepted Manuscript, available also at: <http://arxiv.org/abs/1511.05715>.
- 470 [21] C. Hofer, U. Langer, and I. Touloupoulos. Discontinuous Galerkin Isoge-  
471 ometric Analysis on non-matching segmentation: error estimates and efficient  
472 solvers. RICAM-Report 23, Johann Radon Institute for Computational and  
473 Applied Mathematics, Austrian Academy of Sciences, 2016. available at  
474 [https://www.ricam.oeaw.ac.at/publications/ricam-reports/Report No. 2016-23](https://www.ricam.oeaw.ac.at/publications/ricam-reports/Report%20No.%202016-23).
- 475 [22] C. Hofer and I. Touloupoulos. Discontinuous Galerkin Isogeometric Analysis of elliptic  
476 problems on segmentations with non-matching interfaces. *Computers & Mathematics*  
477 *with Applications*, 72(7):1811 – 1827, 2016.
- 478 [23] J. Hoschek and D. Lasser. *Fundamentals of Computer Aided Geometric Design*. A  
479 K Peters, Wellesley, Massachusetts, 1993. Translated by L. Schumaker.

- 480 [24] T. J. R. Hughes, J. A. Cottrell, and Y. Bazilevs. Isogeometric analysis: CAD, finite  
481 elements, NURBS, exact geometry and mesh refinement. *Comput. Methods Appl.  
482 Mech. Engrg.*, 194:4135–4195, 2005.
- 483 [25] B. Jüttler, M. Kapl, D.-M. Nguyen, Q. Pan, and M. Pauley. Isogeometric segmen-  
484 tation: The case of contractible solids without non-convex edges. *Computer-Aided  
485 Design*, 57:74–90, 2014.
- 486 [26] A. Klawonn, M. Lanser, and O. Rheinbach. Nonlinear FETI-DP and BDDC methods.  
487 *SIAM J. Sci. Comput.*, 36(2):737–765, 2014.
- 488 [27] A. Klawonn, M. Lanser, and O. Rheinbach. Toward extremely scalable nonlinear  
489 domain decomposition methods for elliptic partial differential equations. *SIAM J.  
490 Sci. Comput.*, 37(6):c667–c696, 2015.
- 491 [28] A. Klawonn, M. Lanser, and O. Rheinbach. A nonlinear FETI-DP method with an  
492 inexact coarse problem. In *Domain decomposition methods in science and engineering  
493 XXII. Proceedings of the 22nd international conference on domain decomposition  
494 methods, Lugano, Switzerland, September 16–20, 2013*, pages 41–52. Cham: Springer,  
495 2016.
- 496 [29] A. Klawonn, M. Lanser, O. Rheinbach, H. Stengel, and G. Wellein. *Hybrid  
497 MPI/OpenMP Parallelization in FETI-DP Methods*, pages 67–84. Springer Inter-  
498 national Publishing, Cham, 2015.
- 499 [30] A. Klawonn and O. Rheinbach. A parallel implementation of Dual-Primal FETI  
500 methods for three-dimensional linear elasticity using a transformation of basis. *SIAM  
501 Journal on Scientific Computing*, 28(5):1886–1906, 2006.
- 502 [31] A. Klawonn and O. Rheinbach. Inexact FETI-DP methods. *International journal  
503 for numerical methods in engineering*, 69(2):284–307, 2007.
- 504 [32] A. Klawonn and O. Rheinbach. Highly scalable parallel domain decomposition meth-  
505 ods with an application to biomechanics. *ZAMM - Journal of Applied Mathematics  
506 and Mechanics / Zeitschrift für Angewandte Mathematik und Mechanik*, 90(1):5–32,  
507 2010.
- 508 [33] A. Klawonn, O. Rheinbach, and L. F. Pavarino. Exact and inexact FETI-DP methods  
509 for spectral elements in two dimensions. In *Domain decomposition methods in science  
510 and engineering XVII. Selected papers based on the presentations at the 17th inter-  
511 national conference on domain decomposition methods, St. Wolfgang/Strobl, Austria,  
512 July 3–7, 2006.*, pages 279–286. Berlin: Springer, 2008.
- 513 [34] S. Kleiss, C. Pechstein, B. Jüttler, and S. Tomar. IETI–isogeometric tearing and  
514 interconnecting. *Computer Methods in Applied Mechanics and Engineering*, 247:201–  
515 215, 2012.
- 516 [35] A. Kuzmin, M. Luisier, and O. Schenk. Fast methods for computing selected ele-  
517 ments of the greens function in massively parallel nanoelectronic device simulations.  
518 In F. Wolf, B. Mohr, and D. Mey, editors, *Euro-Par 2013 Parallel Processing*, vol-  
519 ume 8097 of *Lecture Notes in Computer Science*, pages 533–544. Springer Berlin  
520 Heidelberg, 2013.

- 521 [36] U. Langer, A. Mantzaflaris, S. E. Moore, and I. Touloupoulos. Multipatch dis-  
522 continuous Galerkin isogeometric analysis. In B. Jüttler and B. Simeon, editors,  
523 *Isogeometric Analysis and Applications IGAA 2014*, volume 107 of *Lecture Notes*  
524 *in Computer Science*, pages 1–32, Heidelberg, 2015. Springer. also available at  
525 <http://arxiv.org/abs/1411.2478>.
- 526 [37] U. Langer and I. Touloupoulos. Analysis of multipatch discontinuous Galerkin IgA  
527 approximations to elliptic boundary value problems. *Computing and Visualization*  
528 *in Science*, 17(5):217–233, 2015.
- 529 [38] J. Li and O. B. Widlund. On the use of inexact subdomain solvers for BDDC  
530 algorithms. *Comput. Methods Appl. Mech. Eng.*, 196(8):1415–1428, 2007.
- 531 [39] J. Mandel, C. R. Dohrmann, and R. Tezaur. An algebraic theory for primal and dual  
532 substructuring methods by constraints. *Appl. Numer. Math.*, 54(2):167–193, 2005.
- 533 [40] A. Mantzaflaris, C. Hofer, et al. G+Smo (Geometry plus Simulation modules) v0.8.1.  
534 <http://gs.jku.at/gismo>, 2015.
- 535 [41] M. Pauley, D.-M. Nguyen, D. Mayer, J. Speh, O. Weeger, and B. Jüttler. The  
536 isogeometric segmentation pipeline. In B. Jüttler and B. Simeon, editors, *Isogeometric*  
537 *Analysis and Applications IGAA 2014*, Lecture Notes in Computer Science,  
538 Heidelberg, 2015. Springer. to appear, also available as Technical Report no. 31 at  
539 <http://www.gs.jku.at>.
- 540 [42] C. Pechstein. *Finite and boundary element tearing and interconnecting solvers for*  
541 *multiscale problems*. Berlin: Springer, 2013.
- 542 [43] O. Rheinbach. Parallel iterative substructuring in structural mechanics. *Arch. Com-*  
543 *put. Methods Eng.*, 16(4):425–463, 2009.
- 544 [44] B. Rivière. *Discontinuous Galerkin methods for solving elliptic and parabolic equa-*  
545 *tions. Theory and implementation*. Philadelphia, PA: Society for Industrial and Ap-  
546 plied Mathematics (SIAM), 2008.
- 547 [45] A. Toselli and O. B. Widlund. *Domain decomposition methods – algorithms and*  
548 *theory*. Berlin: Springer, 2005.
- 549 [46] X. Tu. Three-level BDDC in three dimensions. *SIAM Journal on Scientific Comput-*  
550 *ing*, 29(4):1759–1780, 2007.
- 551 [47] X. Tu. Three-level BDDC in two dimensions. *International journal for numerical*  
552 *methods in engineering*, 69(1):33–59, 2007.
- 553 [48] S. Zampini. *Inexact BDDC Methods for the Cardiac Bidomain Model*, pages 247–255.  
554 Springer International Publishing, Cham, 2014.